

# Theoretical Study on the Weakly-Bound Complexes in the Reactions of Hydroxyl Radical with Saturated Hydrocarbons (Methane, Ethane, and Propane)

Tomohiro Hashimoto\*

Japan Science and Technology Corporation and Faculty of Regional Studies, Gifu University, Gifu, 501-1193, Japan

Suehiro Iwata

Institute for Molecular Science, Okazaki 444-8585, Japan, Department of Chemistry, Graduate School of Science, Hiroshima University, Higashi-Hiroshima, 739-8526, Japan, and Education and Research Evaluation Division, Faculty of University Evaluation and Research, NIAD, Chiyoda-ku, Tokyo, 101-8438, Japan

Received: August 15, 2001; In Final Form: December 19, 2001

Weakly bound reactant and product complexes in the hydrogen abstraction reactions of an OH radical with CH<sub>4</sub>, C<sub>2</sub>H<sub>6</sub>, and C<sub>3</sub>H<sub>8</sub> are investigated with ab initio molecular orbital methods. The calculated binding energy of the CH<sub>4</sub> and OH reactant complex at CCSD(T)/aug-cc-pVTZ (aug-cc-pVDZ) levels is 0.54 (0.74) kcal/mol. The zero-point vibrational energy correction at MP2 level with the corresponding basis sets reduces the binding energy to 0.16 (0.08) kcal/mol, which is substantially smaller than the recent experimental estimation (about 0.60 kcal/mol). A product complex for the CH<sub>4</sub> + OH system, which is more stable than the reactant complex, has the binding energy of 0.77 (0.79) kcal/mol at CCSD(T)/aug-cc-pVTZ (aug-cc-pVDZ) levels with MP2 zero-point energy corrections. The reactant and product complexes are also found for the C<sub>2</sub>H<sub>6</sub> + OH and C<sub>3</sub>H<sub>8</sub> + OH reactions at the CCSD(T)/aug-cc-pVDZ level of theory. The binding energies tend to increase with the number of carbon atoms of the hydrocarbon. The reaction rates and their temperature dependence are estimated, and they are more than 1 order of magnitude larger than the experimentally reported values.

## Introduction

Hydroxyl radical OH is one of the most important reactive chemical species in both the troposphere and the stratosphere of the earth. It is formed through the reactions of water molecules with ozone, and it quickly reacts with the surrounding atmospheric trace gaseous molecules. Such reactions initiate the chains of chemical reactions in the atmosphere. The OH radical has high reactivity toward hydrocarbons, and the reaction of an OH radical with the simplest hydrocarbon, methane, controls the concentration of methane in the troposphere and also that of the OH radical itself. The hydrogen abstraction reactions from saturated hydrocarbons by OH also play important roles in the combustion process. Therefore, several studies on these reactions have been carried out both experimentally<sup>1–5</sup> and theoretically.<sup>6–12</sup> Among them, Tsiouris et al.<sup>3</sup> recently succeeded in identifying the reactant complexes of CH<sub>4</sub> and OH at the entrance channel. They used laser-induced fluorescence and stimulated Raman excitation spectra at low temperature. Their estimated binding energy of a CH<sub>4</sub>···OH complex is as small as 210 ± 20 cm<sup>-1</sup> (0.60 ± 0.06 kcal/mol). In the present work, we theoretically search the weakly bound complexes in this reaction system using ab initio molecular orbital methods and investigate their features if they ever exist. Furthermore, we extend the study to the complexes of OH with the other saturated hydrocarbons (ethane and propane). In all reactions we examined, the slightly stronger complexes of an R···HOH form are found at the exit channel. Using the simple transition state theory, the reaction rates and

their temperature dependence are estimated, and are compared with the experimental values.

## Computational Details

All ab initio calculations in this work are carried out using a GAUSSIAN 98 program package,<sup>13</sup> registered at Computer Center of Institute for Molecular Science and at Hiroshima University. Molecular structures of the complexes and the transition states are optimized at the UMP2 level for the reactions of a hydroxyl radical with a series of hydrocarbons. Electron correlation energy is further taken into account with the UMP4 and CCSD(T) methods at the UMP2 optimum geometries. Harmonic vibrational frequencies for the zero-point energy corrections are computed at the UMP2 level. The augmented correlation consistent basis sets of Dunning and co-workers<sup>14,15</sup> are used: aug-cc-pVDZ (AVDZ) and aug-cc-pVTZ (AVTZ) basis sets for the methane and OH system and AVDZ for both ethane–OH and propane–OH systems. Single-point energy calculations with larger basis sets are also performed: aug-cc-pVQZ (AVQZ) for the methane and OH system, AVTZ for ethane and OH system, and AVTZ without *f*-functions for carbon and oxygen atoms and *d*-functions for hydrogen atoms for propane and OH system. Rate constants are simply evaluated by the conventional transition state theory with zero curvature transmission coefficients<sup>6</sup> using TheRate program.<sup>16</sup>

## Results and Discussions

We have examined the abstraction reactions of an OH radical with three of the simplest saturated hydrocarbons—methane,

\* Corresponding author. Fax: +81-58-293-3008. E-mail: thashi@cc.gifu-u.ac.jp.

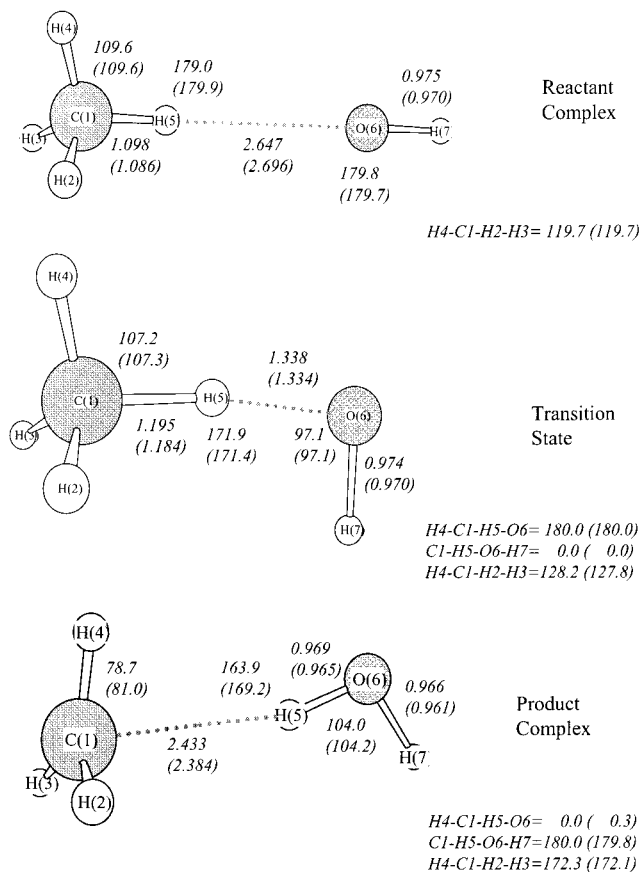


**Figure 1.** Optimized structures of the complexes and the transition state in the reaction of  $\text{CH}_4 + \text{OH} \rightarrow \text{CH}_3 + \text{H}_2\text{O}$  at the UMP2/aug-cc-pVDZ (aug-cc-pVTZ) level. Bond length in Å and angles in degree.

ethane, and propane. The structures of the intermediate complexes and transition states are shown in Figures 1–3, and the energy profiles of the reactions are compared in Figure 4. Tables 1–3 summarize the relative energies, and their basis set and method dependences are also given in the tables.

**CH<sub>4</sub> and OH System.** As Tsiouris et al. suggested in their experimental study, we have succeeded in locating a stable structure of the  $\text{CH}_4$  and OH reactant complex in the entrance channel at the UMP2 level; the structure is shown in Figure 1. Some of the selected geometrical parameters are given in the figure. In the complex, the oxygen atom is located at 2.647 Å away from the nearest hydrogen atom of  $\text{CH}_4$  at the UMP2/AVDZ level of approximation. With the AVTZ basis set, the O(6)–H(5) bond length is 2.696 Å which is slightly longer than that for the AVDZ basis set. The differences of the other geometrical parameters with these two basis sets are much smaller. The bond angles of C(1)–H(5)–O(6) and H(5)–O(6)–H(7) are almost 180°, which means that the four atoms of C(1), H(5), O(6), and H(7) are collinear. It is noted that the structures of both  $\text{CH}_4$  and OH moieties of the complex are almost identical with the corresponding isolated moiety; note that C–H bond lengths of methane are 1.098 (1.086) Å and H–C–H bond angles are 109.5° (109.5°) at the UMP2/AVDZ (AVTZ) level and that the OH bond length of a free hydroxyl radical is 0.975 (0.970) Å. It is consistent with the small binding energy of this complex. The reactant complex is more stable than the reactants only by 0.70 kcal/mol at the UMP2 level, 0.75 kcal/mol at UMP4 level, and 0.74 kcal/mol at CCSD(T) level with AVDZ basis set (see Table 1). The zero-point vibrational energy (ZPVE) correction at the UMP2 level reduces the binding energy to be only less than 0.1 kcal/mol. The extension of the basis

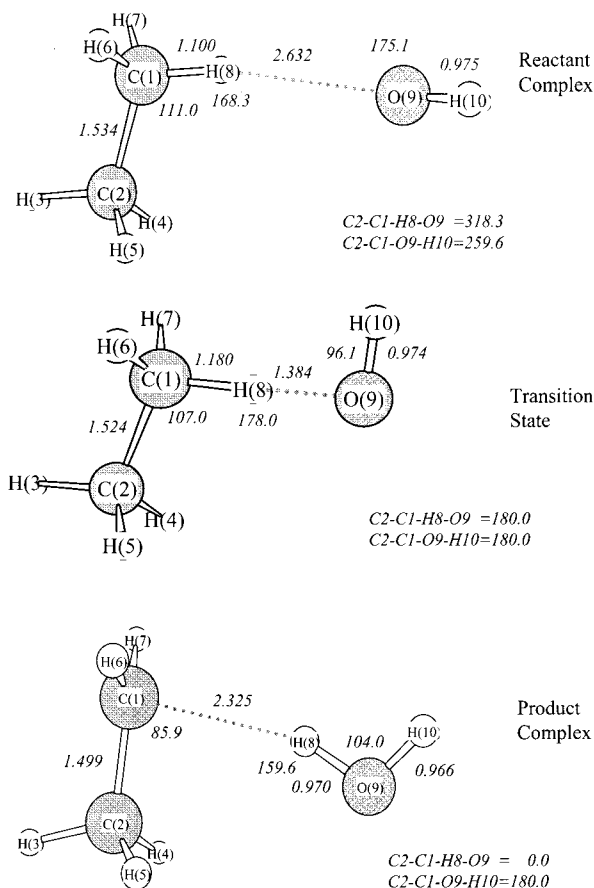


**Figure 2.** Optimized structures of the complexes and the transition state in the reaction of  $\text{C}_2\text{H}_6 + \text{OH} \rightarrow \text{C}_2\text{H}_5 + \text{H}_2\text{O}$  at the UMP2/aug-cc-pVDZ level. Bond length in Å and angles in degree.

set to the AVTZ set decreases the binding energies further by 0.20 kcal/mol without the ZPVE correction, and it doubles the energy with the ZPVE correction. The CCSD(T) binding energies using aug-cc-pVTZ are 0.54 and 0.16 kcal/mol with and without ZPVE correction, respectively. The electron correlation effect on the binding energy of the reactant complex converges at the CCSD(T) level, while the basis set limit of one-electron functions is not yet reached in the AVTZ level. Due to the poor convergence to the basis set limit, we performed a single-point energy calculation using AVQZ at the optimum UMP2/AVTZ geometry. The calculated binding energies become smaller than those with AVTZ and are 0.43 kcal/mol at UMP2, 0.46 kcal/mol at UMP4, and 0.46 kcal/mol at CCSD(T) level. The convergence of the electron correlation effect is observed again in these calculations. The difference of binding energy between AVQZ and AVTZ values (0.08 kcal/mol at CCSD(T) level) becomes less than half as much as that between AVTZ and AVDZ values (0.20 kcal/mol at CCSD(T) level). Because this difference between AVQZ and AVTZ values is about 15% of AVTZ binding energy, we may not claim the convergence of basis set effect, though the relaxation of molecular structures is not taken into account with the AVQZ set. The basis set superposition error (BSSE) might play a role. Our recent study on the basis set dependence of the BSSE indicates that the diffuse augmented functions substantially reduce the BSSE for a series of VXZ basis sets (X = D, T, and Q).<sup>17</sup> It is particularly true for the AVQZ and AV5Z basis sets. Thus, our best estimated binding energy is 0.2 and 0.5 kcal/mol with and without the ZPVE, respectively. It does apparently underestimate the experimentally determined value,  $0.60 \pm 0.06$  kcal/mol. The basis set deficiency is one of the reasons for the

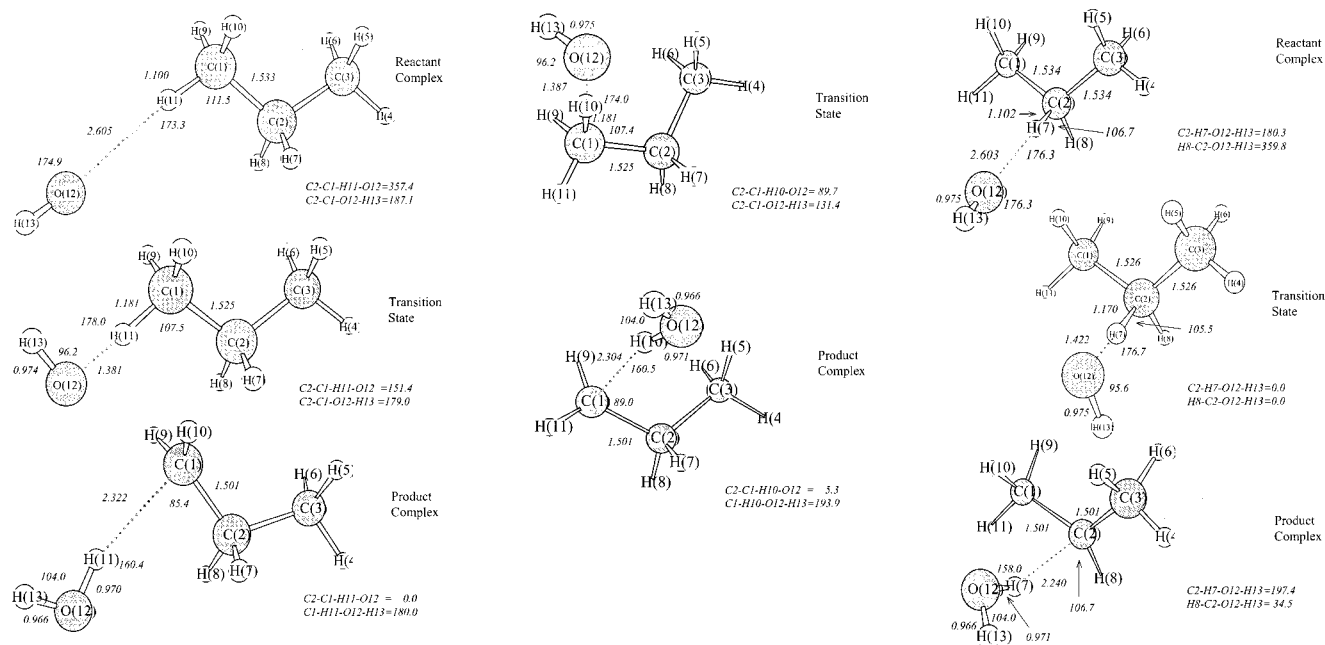


**Figure 3.** Optimized structures of the complexes and the transition state in the reaction of  $C_3H_8 + OH \rightarrow C_3H_7 + H_2O$  at the UMP2/aug-cc-pVDZ level. (a) Primary site 1, (b) primary site 2, (c) secondary site. Bond length in Å and angles in degree.

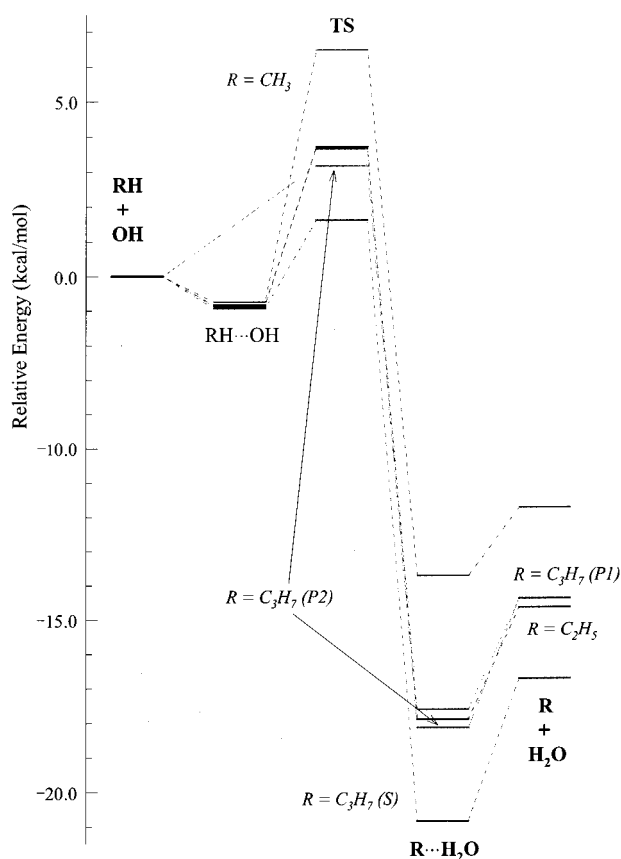


**Figure 4.** Energy profiles of  $RH + OH \rightarrow R + H_2O$  ( $R = CH_3, C_2H_5, C_3H_7$ ) at the CCSD(T)/aug-cc-pVDZ//UMP2/aug-cc-pVDZ level.

error, and the other possibility might be the harmonic approximation of the ZPVE.

We have also located the product complex of  $CH_3 \cdots H_2O$  in the reaction, whose structure is shown in the bottom of Figure 1. The distance between C(1) and H(5) is 2.433 Å, which becomes slightly shorter (by 0.049) with the AVTZ basis set. In the product complex, the four atoms, C(1), H(5), O(6), and

H(7), are still on the same plane, but the atoms no longer lie collinearly. The angles,  $C(1)-H(5)-O(6)$  and  $H(4)-C(1)-H(5)$ , are slightly basis-set-dependent as shown in the figure. The geometric structures of two moieties are slightly different from those of a free methyl radical and of a water molecule; the  $CH_3 \cdots H_2O$  complex is more stable than the product by 1.91 kcal/mol at the UMP2 level, 2.01 kcal/mol at the UMP4 level, and 1.99 kcal/mol at the CCSD(T) level with AVDZ basis set. The ZPVE correction reduces these values by about 1.2 kcal/mol. The binding energies calculated with the AVTZ basis set are 1.84 (0.69) kcal/mol at UMP2 level, 1.93 (0.78) kcal/mol at UMP4 level, and 1.92 (0.77) kcal/mol at CCSD(T) level without (with) UMP2 ZPVE correction. Thus, AVTZ values are smaller by about 0.07 (0.02) kcal/mol than AVDZ values. It is noted that the influence of the extension of the basis set from AVDZ to AVTZ on the calculated binding energies is different between the reactant complex and the product complex, especially for ZPVE corrected energies. The binding energies by the single-point energy calculations with the AVQZ basis set are 1.72 kcal/mol at UMP2, 1.79 kcal/mol at UMP4, and 1.78 kcal/mol at CCSD(T) level. The difference between AVQZ and AVTZ values are about twice as much as that between the AVTZ and AVDZ values. This may be due to taking no account of the structural relaxation. The UMP4 and CCSD(T) values are almost the same as seen in the case of the reactant complex, which indicates that the electron correlation effect on the binding energy of the product complex has converged at the CCSD(T) level of theory.

**$C_2H_6$  and OH System.** The corresponding reactant and product complexes in  $C_2H_6 + OH \rightarrow C_2H_5 + H_2O$  reaction system are examined. The equilibrium structures of these complexes are shown in Figure 2. The relative energies with respect to the reactants are listed in Table 2, and the energy profile is compared in Figure 4 with the other reactions. As in the  $CH_4 \cdots OH$  reactant complex, the structures of the two moieties (top in Figure 2) are almost identical with those of an

**TABLE 1: Relative Energies (kcal/mol) of the Equilibrium Structures and Transition State for  $\text{CH}_4 + \text{OH} \rightarrow \text{CH}_3 + \text{H}_2\text{O}^a$** 

|   |                   | UMP2            | UMP4            | CCSD(T)         |
|---|-------------------|-----------------|-----------------|-----------------|
| $\text{CH}_4 + \text{OH}$               |                   | 0.00 (0.00)     | 0.00 (0.00)     | 0.00 (0.00)     |
| $\text{CH}_4 \cdots \text{OH}$          | AVDZ <sup>b</sup> | -0.70 (-0.04)   | -0.75 (-0.09)   | -0.74 (-0.08)   |
|   | AVTZ <sup>b</sup> | -0.49 (-0.11)   | -0.55 (-0.17)   | -0.54 (-0.16)   |
|   | AVQZ <sup>c</sup> | -0.43           | -0.46           | -0.46           |
| TS                                      | AVDZ              | 8.21 (6.79)     | 7.84 (6.42)     | 6.48 (5.06)     |
|   | AVTZ              | 8.20 (6.72)     | 7.59 (6.11)     | 6.43 (4.95)     |
|   | AVQZ              | 8.15            | 7.53            | 6.35            |
| $\text{CH}_3 \cdots \text{H}_2\text{O}$ | AVDZ              | -18.15 (-18.26) | -14.29 (-14.40) | -13.73 (-13.84) |
|   | AVTZ              | -18.48 (-18.84) | -14.92 (-15.28) | -14.15 (-14.51) |
|   | AVQZ              | -19.08          | -15.55          | -14.76          |
| $\text{CH}_3 + \text{H}_2\text{O}$      | AVDZ              | -16.24 (-17.55) | -12.28 (-13.59) | -11.74 (-13.05) |
|   | AVTZ              | -16.64 (-18.15) | -12.99 (-14.50) | -12.23 (-13.74) |
|   | AVQZ              | -17.36          | -13.76          | -12.98          |

<sup>a</sup> Values in parentheses are the UMP2 zero-point vibrational energy corrected energies. UMP4 and CCSD(T) calculations were performed at optimum UMP2 geometries. <sup>b</sup> AVDZ and AVTZ stand for Dunning's aug-cc-pVDZ and aug-cc-pVTZ basis set, respectively. <sup>c</sup> Single-point energy calculations at UMP2/AVDZ geometries with Dunning's aug-cc-pVQZ basis set.

**TABLE 2: Relative Energies (kcal/mol) of the Equilibrium Structures and Transition State for  $\text{C}_2\text{H}_6 + \text{OH} \rightarrow \text{C}_2\text{H}_5 + \text{H}_2\text{O}^a$** 

|  |                   | UMP2            | UMP4            | CCSD(T)         |
|--|-------------------|-----------------|-----------------|-----------------|
| $\text{C}_2\text{H}_6 + \text{OH}$               |                   | 0.00 (0.00)     | 0.00 (0.00)     | 0.00 (0.00)     |
| $\text{C}_2\text{H}_6 \cdots \text{OH}$          | AVDZ <sup>b</sup> | -0.77 (-0.24)   | -0.84 (-0.31)   | -0.83 (-0.30)   |
|  | AVTZ <sup>c</sup> | -0.55           | -0.60           | -0.59           |
| TS   | AVDZ              | 5.79 (4.11)     | 5.26 (3.58)     | 3.70 (2.02)     |
|  | AVTZ              | 5.87            | 5.14            | 3.72            |
| $\text{C}_2\text{H}_5 \cdots \text{H}_2\text{O}$ | AVDZ              | -22.03 (-22.06) | -18.36 (-18.39) | -17.90 (-17.93) |
|  | AVTZ              | -22.48          | -19.10          | -18.44          |
| $\text{C}_2\text{H}_5 + \text{H}_2\text{O}$      | AVDZ              | -18.81 (-20.31) | -15.06 (-16.56) | -14.65 (-16.15) |
|  | AVTZ              | -19.61          | -16.17          | -15.54          |

<sup>a</sup> Values in parentheses are the UMP2 zero-point vibrational energy corrected energies. UMP4 and CCSD(T) calculations were performed at optimum UMP2 geometries. <sup>b</sup> Dunning's aug-cc-pVDZ basis set. <sup>c</sup> Single-point energy calculations at UMP2/AVDZ geometries with Dunning's aug-cc-pVTZ basis set.

**TABLE 3: Relative Energies (kcal/mol) of the Equilibrium Structures and Transition State for  $\text{C}_3\text{H}_8 + \text{OH} \rightarrow \text{C}_3\text{H}_7 + \text{H}_2\text{O}^a$** 

|   |                   | UMP2            | UMP4            | CCSD(T)         |
|---|-------------------|-----------------|-----------------|-----------------|
| $\text{C}_3\text{H}_8 + \text{OH}$                    |                   | 0.00 (0.00)     | 0.00 (0.00)     | 0.00 (0.00)     |
| $\text{C}_3\text{H}_8 \cdots \text{OH}$ (P1)          | AVDZ <sup>b</sup> | -0.80 (-0.37)   | -0.88 (-0.45)   | -0.87 (-0.44)   |
|   | AVTZ <sup>c</sup> | -0.50           | -0.57           | -0.56           |
| (P2)  |                   |                 |                 |                 |
|   | (S)               | AVDZ            | -0.87 (-0.12)   | -0.94 (-0.19)   |
| TS (P1)   | AVDZ              | 5.78 (4.00)     | 5.21 (3.43)     | 3.65 (1.87)     |
|   | AVTZ              | 6.69            | 5.92            | 4.54            |
| (P2)  | AVDZ              | 5.33 (3.66)     | 4.73 (3.06)     | 3.16 (1.49)     |
|   | AVTZ              | 6.32            | 5.52            | 4.12            |
| (S)   | AVDZ              | 3.93 (2.29)     | 3.29 (1.65)     | 1.61 (-0.03)    |
|   | AVTZ              | 4.87            | 4.05            | 2.54            |
| $\text{C}_3\text{H}_7 \cdots \text{H}_2\text{O}$ (P1) | AVDZ              | -21.55 (-21.32) | -18.01 (-17.78) | -17.61 (-17.38) |
|   | AVTZ              | -20.81          | -17.53          | -16.92          |
| (P2)  | AVDZ              | -22.15 (-22.04) | -18.57 (-18.46) | -18.14 (-18.03) |
|   | AVTZ              | -21.39          | -18.08          | -17.44          |
| (S)   | AVDZ              | -24.74 (-24.59) | -21.26 (-21.11) | -20.86 (-20.71) |
|   | AVTZ              | -24.14          | -20.92          | -20.31          |
| $\text{C}_3\text{H}_7 + \text{H}_2\text{O}$ (P)       | AVDZ              | -18.44 (-19.79) | -14.76 (-16.11) | -14.39 (-15.74) |
|   | AVTZ              | -18.23          | -14.82          | -14.24          |
| (S)   | AVDZ              | -20.59 (-22.05) | -17.03 (-18.49) | -16.72 (-18.18) |
|   | AVTZ              | -20.69          | -17.41          | -16.87          |

<sup>a</sup>Using Dunning's aug-cc-pVDZ basis set. P1, P2, and S in the first column correspond to primary site 1, primary site 2, and secondary site, respectively. Values in parentheses are the UMP2 zero-point vibrational energy corrected energies. UMP4 and CCSD(T) calculations were performed at optimum UMP2 geometries. <sup>b</sup> Dunning's aug-cc-pVDZ basis set. <sup>c</sup> Single-point energy calculations at UMP2/AVDZ geometries with Dunning's aug-cc-pVTZ basis set without *f*-functions for carbon and oxygen atoms, and *d*-functions for hydrogen atoms.

isolated ethane and of a hydroxyl radical. However, the atoms, C(1)–H(8)–O(9), are no more collinear, and the bond O(9)–H(10) is slightly out-of-plane of C(1)–H(8)–O(9). The H(8)–

O(9) distance is 2.632 Å, which is slightly shorter than the corresponding length in the  $\text{CH}_4 \cdots \text{OH}$  complex. At the same level of approximation, the calculated binding energies of the



$C_2H_6\cdots OH$  reactant complex are larger than those of the  $CH_4\cdots OH$  complex by 10% without the ZPVE correction. The UMP2 ZPVE corrected binding energies of the  $C_2H_6\cdots OH$  complex are larger by about 0.2 kcal/mol than those of the  $CH_4\cdots OH$  complex. The CCSD(T)/AVDZ value is 0.83 kcal/mol. The ZPVE corrected value is 0.30 kcal/mol, which is about four times as much as the corresponding energy of the  $CH_4\cdots OH$  complex. Single-point energy calculations with the AVTZ basis set are also performed to investigate the basis set dependence. The calculated binding energies are 0.55 kcal/mol at UMP2, 0.60 kcal/mol at UMP4, and 0.59 kcal/mol at CCSD(T) level. Thus, the AVTZ values are smaller by 0.22–0.24 kcal/mol than the AVDZ values as it is to the  $CH_4\cdots OH$  complex. The difference between the UMP4 and CCSD(T) values is only 0.01 kcal/mol which indicates the convergence of electron correlation effect.

The bottom of Figure 2 shows the optimized structure of the product complex. The distance between the two components is 2.325 Å. Similarly to the  $CH_3\cdots H_2O$  product complex, the structures of two moieties of the product complex are somewhat deformed from the free product molecules. In this complex, the four atoms of C(1), H(8), O(9), and H(10) are on the same plane. The binding energies of the  $C_2H_5\cdots H_2O$  product complex are computed to be 3.22 kcal/mol at UMP2, 3.30 kcal/mol at UMP4, and 3.25 kcal/mol at the CCSD(T) level with the AVDZ basis set. The UMP2 ZPVE correction decreases them to be 1.75, 1.83, and 1.78 kcal/mol, respectively. The  $C_2H_5\cdots H_2O$  complex has a larger binding energy than the  $CH_3\cdots H_2O$  complex by 1.3 and 1.0 kcal/mol without and with the ZPVE correction at the CCSD(T)/AVDZ level. The extension of the basis set to AVTZ reduces the binding energies to be 2.87 kcal/mol at UMP2, 2.93 kcal/mol at UMP4, and 2.90 kcal/mol at the CCSD(T) level. The AVTZ values are smaller by about 0.35 kcal/mol than the AVDZ values, and the poor convergence of the basis set effect is again found. The deviation from the UMP2 value is 0.03 kcal/mol.

**$C_3H_8$  and OH System.** There are three hydrogen abstraction sites in a propane molecule; they are primary site 1 (P1), primary site 2 (P2), and secondary site (S), whose corresponding reactant and product complexes found in this work are shown in Figure 3a–c. The relative energies with respect to the reactants are summarized in Table 3 and in Figure 4. At the primary site 1, the OH radical attacks to a hydrogen atom of the nearly in-plane position of three carbon atoms. During the reaction path, this planarity almost holds as shown in Figure 3a. The OH radical is bound at 2.605 Å away from P1 hydrogen H(11) in the P1 reactant complex. It is shorter by 0.04 Å than the corresponding length of the  $CH_4\cdots OH$  complex and by 0.03 Å than that of the  $C_2H_6\cdots OH$  complex. The angle C(1)–H(11)–O(12) is slightly bent and the H(13) of OH radical is slightly out-of-plane of C(1)–H(11)–O(12), as in the  $C_2H_6\cdots OH$  complex. On the other hand, in the P1 product complex the planarity of the four atoms of C(1), H(11), O(12), and H(13) is well satisfied. The distance between the two components is 2.322 Å, which is shorter by 0.1 Å than that of the  $CH_3\cdots H_2O$  complex and almost equal to that of the  $C_2H_5\cdots H_2O$  complex. The calculated binding energies of P1 reactant and product complexes at the CCSD(T)/AVDZ level are 0.87 and 3.22 kcal/mol, respectively. With the UMP2 ZPVE correction, the reactant complex has a binding energy of 0.44 kcal/mol, which is more than five times larger than that of the  $CH_4$  and OH, and about one and a half times that of the  $C_2H_6$  and OH system. Note that the largest ZPVE corrected binding energies for reactant complexes are found in the P1 complex. For the product

complex, ZPVE corrected binding energy is 1.64 kcal/mol, which is smaller by 0.14 kcal/mol than that of the  $C_2H_5$  and  $H_2O$  system. The product complex has a binding energy about four times that of the corresponding reactant complex. The enlargement of the basis set to AVTZ (without *f*-functions for carbon and oxygen atoms, and *d*-functions for hydrogen atoms) reduces the binding energies by about 0.3 kcal/mol for the reactant complex and about 0.5 kcal/mol for the product complex. The CCSD(T)/AVTZ values are 0.56 and 2.68 kcal/mol, respectively.

If the OH radical approaches perpendicularly the plane of three carbon atoms at the end carbon C(1) as the P2 path, no reactant complex is found in our work, which is different from the other abstraction reactions. The optimized structure of the P2 product complex is shown in Figure 3b. The H(10) atom of the  $H_2O$  component is 2.304 Å away from the C(1) atom of the  $C_3H_7$  component. The planarity around the abstraction is not satisfied in contrast to the P1 product complex. The binding energies of the P2 product complex are larger by 0.5–0.7 kcal/mol than those of the P1 product complex. The binding energies with the CCSD(T)/AVDZ level are 3.75 and 2.29 kcal/mol without and with the UMP2 ZPVE correction, respectively. The binding energy with AVTZ basis set is smaller by about 0.5 kcal/mol than that with AVDZ and is computed to be 3.20 kcal/mol at the CCSD(T) level.

In reaction path S, the OH radical abstracts one of the hydrogen atoms of the secondary carbon. Figure 3c shows the optimized structures of the reactant (top) and product (bottom) complexes. The distance between  $C_3H_8$  and OH moieties is 2.603 Å, almost the same as that of the P1 reactant complex. The planarity around the reaction site (H(8)–C(2)–H(7)–O(12)–H(13)) is almost satisfied in this complex, and four atoms, C(2), H(7), O(12), and H(13), are aligned more linearly than the corresponding atoms in the  $C_2H_6\cdots OH$  and P1 reactant complexes. The binding energies without the ZPVE corrections of this complex are the largest among the reactant complexes studied in this work. The calculated values using the AVDZ basis set are 0.87 kcal/mol at the UMP2 level, 0.94 kcal/mol at the UMP4 level, and 0.93 kcal/mol at the CCSD(T) level. They are larger by about 0.2 kcal/mol than the corresponding ones of  $CH_4\cdots OH$ . However, the UMP2 ZPVE corrected energies are only one-third those of the P1 reactant complex at the UMP2 level (0.12 kcal/mol) and less than a half at the CCSD(T) level (0.18 kcal/mol). The enlargement of the basis set to AVTZ reduced the binding energy by 0.3 kcal/mol. The CCSD(T)/AVTZ method computes it to be 0.63 kcal/mol. The distance between the two moieties of the S product complex is 2.240 Å, which is the shortest among the complexes in this work. Contrary to the S reactant complex, the S product complex does not have a symmetry plane, thus the atoms around the reaction site are no longer on the same plane. The largest binding energies of the product complexes both with and without UMP2 ZPVE corrections are found in the S product complex. The CCSD(T)/AVDZ method estimates the binding energy to be 4.15 and 2.54 kcal/mol without and with the ZPVE correction, respectively. Using the AVTZ basis set, the calculated binding energies are smaller by 0.7 kcal/mol than the corresponding AVDZ values. The CCSD(T)/AVTZ energy without the ZPVE correction value is 3.44 kcal/mol. The difference between the UMP2, UMP4, and CCSD(T) binding energies of the product complex are within 0.1 kcal/mol. Again, they are less dependent on the level of the electron correlation.

**Features of Hydrogen Abstraction from Hydrocarbons by an OH Radical.** The transition states (TS) structures for the

**TABLE 4: Rate Constants ( $k$  in  $\text{cm}^3 \text{ molecule}^{-1} \text{ s}^{-1}$ ) for  $\text{RH} + \text{OH} \rightarrow \text{R} + \text{H}_2\text{O}$  ( $\text{R} = \text{CH}_3, \text{C}_2\text{H}_5, \text{C}_3\text{H}_7$ ) for the Temperature Range from 200 K to 310 K**

| T(K) | $k$ ( $\text{cm}^3 \text{ molecule}^{-1} \text{ s}^{-1}$ ) <sup>a</sup> |                     |                                   |                     |  |           |                     |  |                     |
|------|---|---------------------|-----------------------------------|---------------------|--|-----------|---------------------|--|---------------------|
|      | R = CH <sub>3</sub>   |                     | R = C <sub>2</sub> H <sub>5</sub> |                     | R = C <sub>3</sub> H <sub>7</sub> (primary site) |           |                     | R = C <sub>3</sub> H <sub>7</sub> (secondary site) |                     |
|      | calc.   | exptl. <sup>b</sup> | calc.                             | exptl. <sup>c</sup> | calc.(P1)  | calc.(P2) | exptl. <sup>d</sup> | calc.  | exptl. <sup>d</sup> |
| 200  | 1.56E-14  |                     | 3.08E-13                          |                     | 4.42E-13   | 1.78E-13  |                     | 5.95E-12   |                     |
| 210  | 1.81E-14  |                     | 3.47E-13                          | 5.22E-14            | 5.00E-13   | 1.96E-13  |                     | 6.19E-12   |                     |
| 220  | 2.10E-14  | 9.25E-16(223 K)     | 3.88E-13                          | 7.42E-14(225 K)     | 5.63E-13   | 2.15E-13  |                     | 6.44E-12   |                     |
| 230  | 2.44E-14  | 1.26E-15(233 K)     | 4.33E-13                          |                     | 6.32E-13   | 2.35E-13  |                     | 6.70E-12   |                     |
| 240  | 2.83E-14  | 1.55E-15            | 4.81E-13                          | 1.01E-13            | 7.05E-13   | 2.56E-13  |                     | 6.97E-12   |                     |
| 250  | 3.29E-14  | 2.05E-15            | 5.33E-13                          | 1.22E-13            | 7.84E-13   | 2.78E-13  |                     | 7.24E-12   |                     |
| 260  | 3.81E-14  |                     | 5.88E-13                          |                     | 8.68E-13   | 3.01E-13  |                     | 7.53E-12   |                     |
| 270  | 4.41E-14  | 3.67E-15(273 K)     | 6.47E-13                          | 1.69E-13            | 9.58E-13   | 3.25E-13  |                     | 7.83E-12   |                     |
| 280  | 5.09E-14  |                     | 7.10E-13                          | 1.82E-13(275 K)     | 1.05E-12   | 3.51E-13  |                     | 8.14E-12   |                     |
| 290  | 5.87E-14  | 5.97E-15(295 K)     | 7.76E-13                          | 2.40E-13(295 K)     | 1.16E-12   | 3.77E-13  | 1.55E-13(295 K)     | 8.46E-12   | 7.81E-13(295 K)     |
| 300  | 6.75E-14  | 6.62E-15            | 8.46E-13                          | 2.55E-13            | 1.26E-12   | 4.05E-13  |                     | 8.79E-12   |                     |
| 310  | 7.74E-14  |                     | 9.20E-13                          |                     | 1.38E-12   | 4.34E-13  |                     | 9.13E-12   |                     |

<sup>a</sup> E-14 denotes  $\times 10^{-14}$ . <sup>b</sup> Reference 1. <sup>c</sup> Reference 4. <sup>d</sup> Reference 5.

hydrogen abstractions are also shown in Figures 1–3. As the features of the TS structures are similar to those in the previous studies,<sup>6–12</sup> we do not discuss the details of the structures for each reaction. In general, the OH radical approaches the target hydrogen atom linearly, and the reactant complexes are formed. During the hydrogen abstraction process, the OH is located at a trans position with respect to the C–C bond (C–H bond for methane). The distances between the oxygen atom and the nearest hydrogen of hydrocarbons are about 1.33 Å for CH<sub>4</sub> system, 1.38 Å for C<sub>2</sub>H<sub>6</sub> and the primary site of C<sub>3</sub>H<sub>8</sub> systems, and 1.42 Å for the secondary site of C<sub>3</sub>H<sub>8</sub> system. The H–O–H angles of the TS structures are about 95–97°. The planarity around the reaction site is conserved well through the abstraction process in CH<sub>4</sub>, C<sub>2</sub>H<sub>6</sub>, and the primary site 1 of C<sub>3</sub>H<sub>8</sub> systems. For the secondary site reaction, the planarity is satisfied in the reactant complex and the TS, but the product complex no longer has the symmetry plane as mentioned above.

The relative energies of the TS structures with respect to the reactants are shown in Tables 1–3. Figure 4 illustrates the schematic summary of the energetics of the hydrogen abstraction reactions at the same level of approximation (CCSD(T)/AVDZ//UMP2/AVDZ). The TS structures are more sensitive to the electron correlation effect than the equilibrium structures, and the barrier height becomes smaller as the method improves; The CCSD(T) estimates about 2 kcal/mol smaller barrier height than the UMP2 method. The basis set effect on the barrier height is not so significant except for C<sub>3</sub>H<sub>8</sub> systems, in which the AVTZ values are larger by about 1 kcal/mol than the corresponding AVDZ values. As shown in Figure 4, the order of the barrier heights is CH<sub>4</sub> + OH > C<sub>2</sub>H<sub>6</sub> + OH > P1 > P2 > S, thus the OH radical can abstract a hydrogen atom more easily from larger hydrocarbons and at the secondary carbons. The CH<sub>4</sub> and OH reaction has a larger barrier height by about 4–5 kcal/mol than the S site reaction of C<sub>3</sub>H<sub>8</sub> and OH. The reaction energy also becomes smaller with more accurate methods, since the products are less stabilized than the reactants. The CCSD(T) values are smaller by about 4 kcal/mol than the UMP2 values. The order of the reaction energies is CH<sub>4</sub> + OH < P1 < C<sub>2</sub>H<sub>6</sub> + OH < P2 < S, which also indicates the higher reactivity of OH radical with larger hydrocarbons. The reaction energy of the S site of C<sub>3</sub>H<sub>8</sub> is larger by about 5 kcal/mol than that of the CH<sub>4</sub> and OH reaction. The experimental values for the CH<sub>4</sub> + OH system are 13.27<sup>7</sup> and 13.41 kcal/mol<sup>3</sup>, which are very close to the CCSD(T) values including the ZVPE correction for the products (CH<sub>3</sub> + H<sub>2</sub>O) in Table 1. For the C<sub>2</sub>H<sub>6</sub> + OH system, the experimental value of 17.30 kcal/mol<sup>10</sup> is closer to the calculated values for the product complex rather than to those for the

products (C<sub>2</sub>H<sub>5</sub> + H<sub>2</sub>O) as shown in Table 2. A similar tendency is also observed for the C<sub>3</sub>H<sub>8</sub> + OH system in Table 3. The experiments<sup>12</sup> are 18.6 kcal/mol for the primary site reaction and 19.6 kcal/mol for the secondary site reaction.

We also estimate the approximate reaction rate constants for these saturated hydrocarbons and OH systems with the conventional transition state theory, which includes the tunneling correction by zero-order interpolated approximation to the zero-curvature method.<sup>6</sup> The geometry and harmonic frequencies are those of the UMP2/AVDZ level and the barrier height is at the CCSD(T)/AVDZ level. The temperature range is from 200 to 310 K, which can correspond to that of the troposphere. The calculated results are summarized in Table 4 with some experimental data and plotted in Figure 5. The calculated rate constants substantially overestimate the experimental rate constants for all reaction systems by one order or one-and-a-half order of magnitude. The ratio of the secondary (S) and primary (P1) reaction rates of C<sub>3</sub>H<sub>8</sub> is 1:0.20 in the experiments at 295 K and 1:0.14 in the TST estimation at 290 K, which is reasonable. Similarly, the ratio of the S reaction and CH<sub>4</sub> reaction rates is 1:0.0076 in the experiments and 1:0.0069 in the estimation. On the other hand, the ratio of the S reaction and C<sub>2</sub>H<sub>6</sub> reaction rates is 1:0.31 in the experiments and 1:0.092 in the TST estimation. In the experiments, the reaction rate of C<sub>2</sub>H<sub>6</sub> + OH is larger than that of the reaction at the primary carbons of C<sub>3</sub>H<sub>8</sub> + OH. But, the order of the TST rate constants is CH<sub>4</sub> + OH < C<sub>2</sub>H<sub>6</sub> + OH < P1 < P2 < S, which is consistent with the order of the barrier height, and the hydrogen abstractions from larger hydrocarbons proceed more easily. From the slope of the fitting lines in Figure 5, the order of the activation energies is similar to that of the calculated barrier heights. The TST rate constants are sensible to the barrier heights. As mentioned above, the calculated barrier heights tend to be lowering with the better basis sets and with the better treatments of electron correlation. The lower barriers imply the faster rate constants. Therefore, the overestimation of the TST rate constants might not be due to the error in estimating the barrier height. To estimate the tunneling effects, the Wigner tunneling correction<sup>18</sup> is also tested; the rate constants for the reaction of CH<sub>4</sub> become smaller than those with the zero-curvature correction, which implies that the difference from the experimental values becomes slightly smaller. But, those for the reactions of C<sub>2</sub>H<sub>6</sub> and C<sub>3</sub>H<sub>8</sub> become larger than those with the zero-curvature correction. More sophisticated theoretical studies are required to estimate the reaction rates and their temperature dependence of the reactions. It is particularly

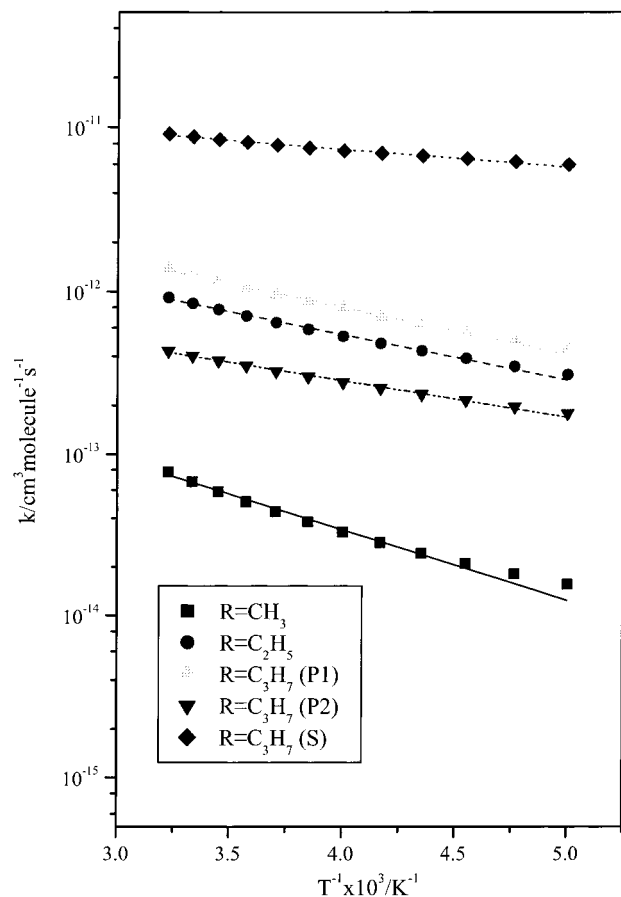


**Figure 5.** The calculated rate constants and their temperature dependence for  $\text{RH} + \text{OH} \rightarrow \text{R} + \text{H}_2\text{O}$  ( $\text{R}=\text{CH}_3, \text{C}_2\text{H}_5, \text{C}_3\text{H}_7$ ).

important to examine the role of the weak reaction complexes at the entrance and exit channels.

### Summary

We found the equilibrium structures of weakly bound complexes in the reactions of hydrogen abstraction from  $\text{CH}_4$  by OH radical. The calculated binding energies of the reactant complex for  $\text{CH}_4$  and OH system with ZPVE corrections are smaller than the experimental estimation. We also found the product complex in the reaction system with larger binding energy than the reactant complex. The reactant and product complexes are also found for  $\text{C}_2\text{H}_6$  and OH system and  $\text{C}_3\text{H}_8$  and OH system. The binding energies become larger as the number of carbon atoms of hydrocarbon increases. The calculated TST rate constants substantially overestimate the reported

experimental constants. The binding energies of these reactant complexes might be too small to have significant effects on the hydrogen abstraction from saturated hydrocarbons in the troposphere, while the corresponding product complexes may have some effects on the following steps, especially for the larger saturated hydrocarbons.

**Acknowledgment.** This work is supported by the project "Computational Chemistry for Molecular Spectroscopies and Chemical Reactions in Atmospheric Environmental Molecules (CCAEM)" of Research and Development Applying Advanced Computational Science and Technology under Japan Science and Technology Corporation. A part of calculations were carried out at the Computer Center of the Institute for Molecular Science.

### References and Notes

- (1) Vaghjiani, G. L.; Ravishankara, A. R. *Nature* **1991**, *350*, 406.
- (2) Gierczak T.; Talukdar, R. K.; Herndon, S. C.; Vaghjiani, G. L.; Ravishankara, A. R. *J. Phys. Chem. A* **1997**, *101*, 3125.
- (3) Tsiouris, M.; Wheeler, M. D.; Lester, M. I. *Chem. Phys. Lett.* **1999**, *302*, 192.
- (4) Talukdar, R. K.; Mellouki, A.; Gierczak, T.; Barone, S.; Chiang, S.-Y.; Ravishankara, A. R. In *1991 Fall Meeting, American Geophysical Union, San Francisco, CA, 1991*; p 101.
- (5) Drooge, A. T.; Tully, F. P. *J. Phys. Chem.* **1986**, *90*, 1949.
- (6) Truong, T. N.; Truhlar, D. G. *J. Chem. Phys.* **1990**, *93*, 1761.
- (7) Melissas, V. S.; Truhlar, D. G. *J. Chem. Phys.* **1993**, *99*, 1013.
- (8) Dobbs, K. D.; Dixon, D. A.; Komornicki, A. *J. Chem. Phys.* **1993**, *98*, 8852.
- (9) Gonzalez, C.; McDouall, J. J.; Schlegel, H. B. *J. Phys. Chem.* **1990**, *94*, 7467.
- (10) Melissas, V. S.; Truhlar, D. G. *J. Phys. Chem.* **1994**, *98*, 875.
- (11) Martell, J. M.; Mehta, A. K.; Pacey, P. D.; Boyd, R. J. *J. Phys. Chem.* **1995**, *99*, 8661.
- (12) Hu, W.-P.; Rossi, I.; Corchado, J. C.; Truhlar, D. G. *J. Phys. Chem. A* **1997**, *101*, 6911.
- (13) Frisch, M. J.; Trucks, G. W.; Schlegel, H. B.; Scuseria, G. E.; Robb, M. A.; Cheeseman, J. R.; Zakrzewski, V. G.; Montgomery, J. A.; Stratmann, R. E.; Burant, J. C.; Dapprich, S.; Millam, J. M.; Daniels, A. D.; Kudin, K. N.; Strain, M. C.; Farkas, O.; Tomasi, J.; Barone, V.; Cossi, M.; Cammi, R.; Mennucci, B.; Pomelli, C.; Adamo, C.; Clifford, S.; Ochterski, J.; Petersson, G. A.; Ayala, P. Y.; Cui, Q.; Morokuma, K.; Malick, D. K.; Rabuck, A. D.; Raghavachari, K.; Foresman, J. B.; Cioslowski, J.; Ortiz, J. V.; Stefanov, B. B.; Liu, G.; Liashenko, A.; Piskorz, P.; Komaromi, I.; Gomperts, R.; Martin, R. L.; Fox, D. J.; Keith, T.; Al-Laham, M. A.; Peng, C. Y.; Nanayakkara, A.; Gonzalez, C.; Challacombe, M.; Gill, P. M. W.; Johnson, B. G.; Chen, W.; Wong, M. W.; Andres, J. L.; Head-Gordon, M.; Replogle, E. S.; Pople, J. A. *Gaussian 98*, Revision A.5; Gaussian, Inc.: Pittsburgh, PA, 1998.
- (14) Dunning, T. H., Jr. *J. Chem. Phys.* **1989**, *90*, 1007.
- (15) Kendall, R. A.; Dunning, T. H., Jr.; Harrison, R. J. *J. Chem. Phys.* **1992**, *96*, 6796.
- (16) *TheRate* program is free software and has been developed by W. T. Duncan and T. N. Truong at the University of Utah. Further information is available at <http://therate.hec.utah.edu/>.
- (17) Nagata, T.; Takahashi, O.; Saito, K.; Iwata, S. *J. Chem. Phys.* **2001**, *115*, 3553.
- (18) Wigner, E. Z. *Phys. Chem.* **1932**, *B19*, 203.